

# Realizing Optimal Current Distributions for Radiation Efficiency in Practical Antennas

Riku Kormilainen , Jari-Matti Hannula , *Member, IEEE*, Tapio O. Saarinen , Anu Lehtovuori ,  
and Ville Viikari , *Senior Member, IEEE*

**Abstract**—Modern antenna design is facing increasing issues with the radiation efficiency, since the space available for antennas is scarce and antennas are fitted into lossy environments. This letter presents a multiport antenna design method with a computationally efficient way to realize the port currents providing the highest radiation efficiency. In this method, an antenna is described with multiple excitation ports in electromagnetic simulations. The measurement results of an example design demonstrate the achieved benefit compared to traditional antenna design.

**Index Terms**—Current, far field, multiport antenna, radiation efficiency.

## I. INTRODUCTION

WITH the advance of wireless communications, antenna designers face increasing challenges. The antennas need to be placed in lossy and challenging environments, and yet their efficiency should be sufficient. This calls for practical antenna structures approaching the ultimate efficiency limits for small antennas. Antenna design is generally done through electromagnetic and circuit simulations where the designer iteratively shapes the antenna structure and possibly tunes an external matching circuit (see, e.g., [1]–[5]). While there are some automated design tools and optimization techniques [6]–[10], practical antenna design relies mainly on the intuition of the antenna designer. Finding the optimal antenna shape may be very challenging and laborious due to high computational burden of electromagnetic simulations and complex relation between antenna shape and its electrical properties. There is no guarantee that the designer can find the optimal solution.

The theoretical and numerical electromagnetics research community, on the other hand, focuses on finding mathematically optimal solutions, and ultimate bounds for the antenna performance. For instance, the famous Chu's limit defines the lower bound for the quality factor of an electrically small antenna [11], and later the approach is extended to find the ultimate efficiency too [12]–[14]. Furthermore, the community has established relatively straightforward ways to solve the ultimately best current or field distributions of an antenna, which would, in certain conditions, result in best possible radiation

properties (see, e.g., [15]–[19]). These methods are attractive as they retrieve the optimal current distribution through optimization with no manual iteration needed. However, incorporating such optimal current distributions into practical antenna design is challenging. First, the calculated antenna structures are often simple in geometry, far from the complicated models of modern wireless devices. Second, the obtained current distribution is difficult to excite in practice, as any practical excitation element easily alters the optimal distribution.

This letter presents a method for designing a practical antenna with port currents optimized for radiation efficiency. Thus, the method is applicable in lossy environments where studying only the impedance properties is not enough. The antenna design procedure is straightforward and does not necessitate manual iteration. This is accomplished by discretizing the antenna structure and solving the discrete current elements. While the theoretical optimization is often performed using the in-house method of moments code, commercial electromagnetic simulators can be used in this approach.

In the following, we introduce the method for modeling the antenna structure in terms of port currents and realizing the optimal currents in the ports, confirm the functionality of the method with a practical prototype and demonstrate the effectiveness of the proposed approach with measurements.

To the authors' knowledge, the proposed antenna design procedure to maximize the radiation efficiency is completely novel. Some previous multiport antenna approaches [20], [21] aiming at certain beam forms as design targets have lead to similar kind of mathematical formulation as the proposed method. The approach in [20] is based on the characteristic basis function method (CBFM) [22]. In CBFM, the radiating region is divided into rectangular patches similar to the proposed procedure. However, the fundamental difference is the definition of the currents. In [22], the discrete currents are related to the current distributions on the divided regions, while in the proposed work the currents are determined at predefined discrete ports (between the patches and between patches and the ground). The proposed method obtains the optimal currents directly from the impedance matrix and port-specific field patterns without a need to construct basis functions as an intermediate result. The proposed method can therefore be considered more straightforward and simpler.

## II. ANTENNA DESIGN PROCEDURE

The steps of the method are shown in Fig. 1. The antenna structure is first discretized into small conductive elements each

Manuscript received January 20, 2020; revised February 17, 2020; accepted February 18, 2020. Date of current version May 5, 2020. The work of R. Kormilainen was supported by the Aalto ELEC Doctoral School. (*Corresponding author: Riku Kormilainen.*)

The authors are with the Department of Electronics and Nano-engineering, Aalto University School of Electrical Engineering, Espoo 02150, Finland (e-mail: riku.kormilainen@aalto.fi; jari-matti.hannula@aalto.fi; tapio.o.saarinen@aalto.fi; anu.lehtovuori@aalto.fi; ville.viikari@aalto.fi).

Digital Object Identifier 10.1109/LAWP.2020.2975668

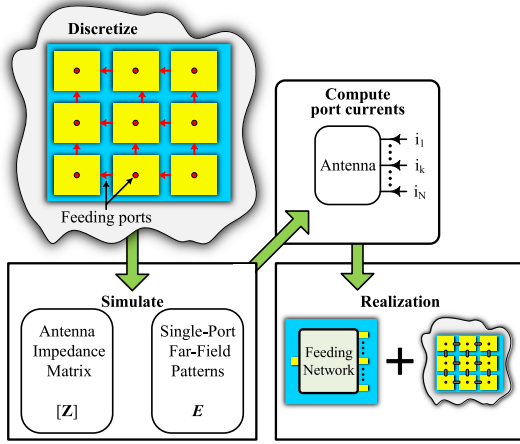


Fig. 1. General diagram showing the steps of the method.

fed with one or more ports. For example, a planar printed circuit board antenna can be discretized into many separate patches, and feeds can be placed both between adjacent patches and between a patch and the ground plane. The second step in the method is to simulate the discretized multiport antenna to obtain the antenna impedance matrix and single-port far-field patterns. Based on the matrix and far-field patterns, the port currents providing the highest radiation efficiency are mathematically solved. Finally, the currents are realized by actively feeding different ports or by replacing ports with reactive loads.

The first step is to construct the far-field pattern as a linear combination of port currents shown in [23]. The far field for an  $N$ -port antenna is

$$\begin{aligned} \vec{F}(\theta, \phi) &= F^\theta(\theta, \phi)\hat{u}_\theta + F^\phi(\theta, \phi)\hat{u}_\phi \\ &= \sum_{k=1}^N \vec{K}_k(\theta, \phi)i_k \\ &= [\vec{K}_1 \cdots \vec{K}_k \cdots \vec{K}_N] [i_1 \cdots i_k \cdots i_N]^T \\ &= \mathbf{K}\mathbf{I} \end{aligned} \quad (1)$$

where  $\vec{K}_k = K_k^\theta(\theta, \phi)\hat{u}_\theta + K_k^\phi(\theta, \phi)\hat{u}_\phi$  maps the current  $i_k$  at port  $k$  to a far-field vector.

After determining the current-far-field-basis  $\mathbf{K}$ , we can compute the radiation efficiency corresponding to any current excitation  $\mathbf{I}$ .

Now the time-averaged power radiated to the far field can be expressed as

$$P_{\text{rad}} = \frac{1}{2\eta_0} \oint_{4\pi} |\vec{F}(\theta, \phi)|^2 d\Omega = \frac{1}{2} \mathbf{I}^H \mathbf{R}_{\text{rad}} \mathbf{I} \quad (2)$$

where  $(\mathbf{R}_{\text{rad}})_{mn} = \frac{1}{\eta_0} \oint_{4\pi} |\vec{K}_m^*(\theta, \phi) \cdot \vec{K}_n(\theta, \phi)|^2$ . The power accepted to the structure is calculated from the port voltages and currents

$$S_{\text{acc}} = \frac{1}{2} \mathbf{U}^H \mathbf{I} = \frac{1}{2} (\mathbf{Z}\mathbf{I})^H \mathbf{I} = \frac{1}{2} \mathbf{I}^H \mathbf{Z}^H \mathbf{I} \quad (3)$$

where  $\mathbf{Z}$  is the impedance matrix of the  $N$ -port antenna. However, only the real part of the power contributes to the radiated

power

$$P_{\text{acc}} = \Re\{S_{\text{acc}}\} = \frac{1}{4} \mathbf{I}^H (\mathbf{Z}^H + \mathbf{Z}) \mathbf{I}. \quad (4)$$

Note that the power accepted does not include matching losses. As a result, the radiation efficiency can be written in terms of the two powers as

$$\eta_{\text{rad}} = \frac{P_{\text{rad}}}{P_{\text{acc}}} = 2 \frac{\mathbf{I}^H \mathbf{R}_{\text{rad}} \mathbf{I}}{\mathbf{I}^H (\mathbf{Z}^H + \mathbf{Z}) \mathbf{I}}. \quad (5)$$

The derived radiation efficiency has a general form of Rayleigh quotient. Thus, the maximum radiation efficiency is obtained by

$$\eta_{\text{rad,max}} = 2 \max\{\text{eig}(\mathbf{R}_{\text{rad}}, \mathbf{Z}^H + \mathbf{Z})\} \quad (6)$$

with the corresponding eigenvector giving the optimal currents. Similar kind of formulation has previously been used for finding the best current distribution for radiation efficiency in an arbitrary structure [8]. However, there are two fundamental differences to our approach. First, the matrix  $\mathbf{Z}$  in the formulation of [8] stands for the surface impedance, whereas it is the port impedance matrix in our analysis. Second, there is no practical way to excite the current distribution found in [8]. This is because any practical excitation element would affect the surface impedance matrix and thus also the optimal current distribution, whereas the excitation elements are inherently included in the port impedance matrix. Note as well that our method makes it possible to limit the number of optimized currents, whereas the number of discrete currents in [8] is proportional to the size of the mesh.

### III. DEMONSTRATION OF THE PROPOSED METHOD

The proposed method is verified through a design of a discretized antenna having port currents calculated with the method. Additionally, the proposed design is manufactured and measured. The objective is to show that the radiation efficiency can be improved by manipulating currents at multiple feeding ports, while retaining the overall shape and size of the antenna. The proposed method is compared to a reference design.

#### A. Reference Antenna

For demonstration purposes, we chose a thin coaxially fed patch antenna operating in 2.4–2.5 GHz band. The reference antenna is shown in Fig. 2. It has a width and length of 43.36 and 29.10 mm, respectively. The substrate is made of FR-4 (Isola 370HR), and the substrate consists of one 0.15 mm thick prepreg ( $\epsilon_r = 3.8$ ,  $\tan \delta = 0.026$ ) slab placed between two 0.71 mm thick ( $\epsilon_r = 4.3$ ,  $\tan \delta = 0.019$ ) core slabs. Overall, the thickness is 1.57 mm. The design consists of three layers: antenna [see Fig. 2(a)], ground [see Fig. 2(c)], and signal layer [see Fig. 2(d)]. The feeding is implemented with a through via, located at the center of the longest edge. The signal layer is connected to the ground with blind vias.

#### B. Design With Optimal Currents

To demonstrate the proposed method, we divide the reference antenna in four symmetrical patches according to Fig. 3. A larger

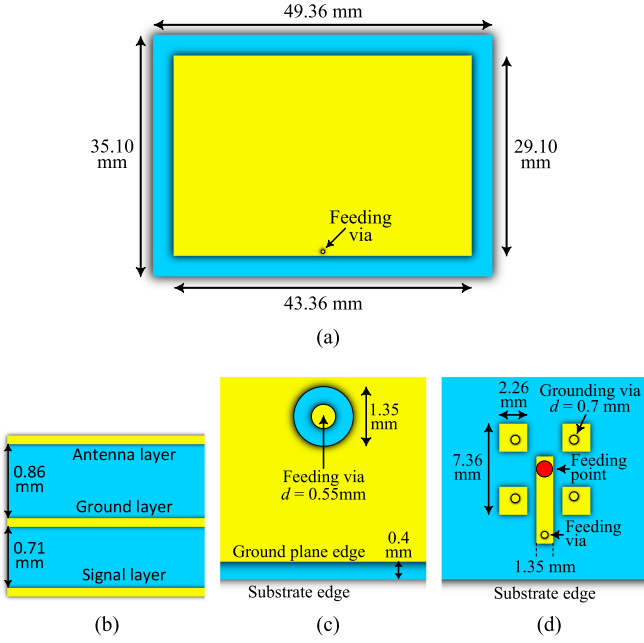


Fig. 2. (a) Top view of the antenna layer. (b) Cross-section of the antenna structure. (c) Close-ups of the feeding via at the ground layer. (d) Connector pad at signal level.

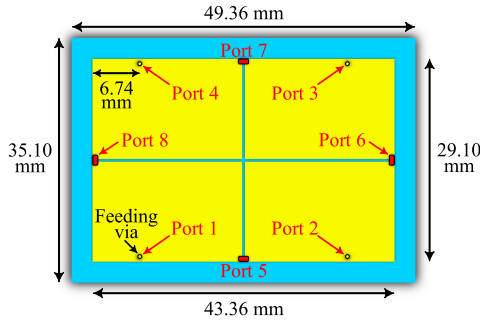


Fig. 3. Antenna layer for the proposed antenna. Other layers are similar to the reference antenna.

number of sections might result in higher efficiency, but would also lead to a more complex structure. The number of patches is selected as a tradeoff between the achievable efficiency and complexity of the structure. The separation between patches is 0.4 mm, and the proposed antenna has eight feeding ports in total. The feeding ports 1–4 are implemented with through vias similar to the reference case. Ports 5–8 are modeled as discrete face ports between the patches. Ports 5–8 were chosen to be at the edges of the patch where the most significant currents tend to lie. Ports 1–4 were first placed at the middle of the patch edges as in the case of the reference antenna. Then, the port locations were shifted toward the outer corners to achieve better matching.

First, the proposed antenna is simulated to obtain far fields  $\vec{E}_k$  and antenna impedance parameters  $\mathbf{Z}$ . Furthermore, these far fields are used to determine the vector  $\mathbf{K}$  for each frequency and angle. Finally, the optimal currents can be solved as an eigenvalue problem from (5).

TABLE I  
PORT TYPES, CURRENTS, AND REALIZATIONS

Port	Type	Current ( $i_k/i_1$ )	Realization
1, 4	active	$1.0\angle 0.0^\circ$	$50\ \Omega$ signal port
2, 3	active	$1.0\angle 180.0^\circ$	$50\ \Omega$ signal port
5, 7	passive	$15.4\angle 19.7^\circ$	1.16 pF capacitor
6, 8	passive	$0.001\angle -16.1^\circ$	open

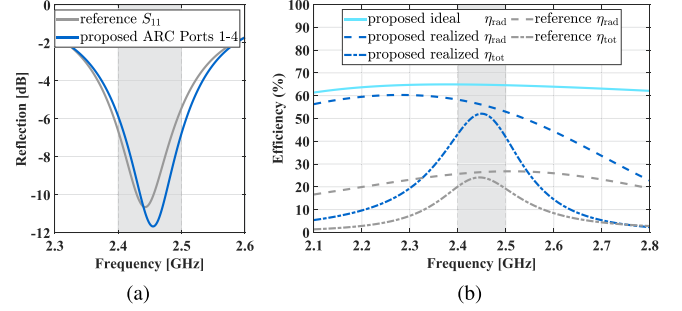


Fig. 4. (a) Simulated reflection coefficient of the reference antenna and ARCs of the proposed antenna. (b) Simulated radiation  $\eta_{\text{rad}}$  and total efficiencies  $\eta_{\text{tot}}$  of the reference and proposed antennas. Additionally, the theoretical maximum for radiation efficiency is shown.

As an example, the computed port currents at 2.45 GHz are shown in Table I. The currents at ports 1–4 have an equal amplitude, but  $180^\circ$  phase difference between ports 1 and 4 and ports 2 and 3. Ports 6 and 8 have almost zero currents, whereas ports 5 and 7 have nonzero currents.

Realization is designed based on optimal currents shown in Table I. Active ports 1–4 are realized with  $50\ \Omega$  sources, which causes some mismatch. As the port impedance is purely real, the relative magnitudes and phases of the ports remain the same as for the currents. Ports 6 and 8 can be left open, since the port currents are practically zero. Passive ports 5 and 7 are realized with lumped elements. By calculating the ports voltages from  $\mathbf{Z}$  with the optimized currents, the required termination impedances can be found. The optimal current would be realized with termination impedances of  $56.11\angle -93.6^\circ\ \Omega$ . Because the impedance is mainly capacitive, they are approximated as ideal 1.16 pF capacitors. In the prototype, the capacitors are real Murata components (series GJM1555C\*) with a nominal value of 1.3 pF, accounting for the nonidealities of the component.

## IV. RESULTS

### A. Simulated Results

Fig. 4(a) shows the reflection coefficient of the reference antenna and the active reflection coefficients (ARCs) of the ports. The reflection coefficients are very similar but they both have a slight offset from the center frequency. The reason is that both designs are optimized for minimum efficiency in the band, which is evident from Fig. 4(b) showing the simulated radiation and total efficiencies of the reference and proposed design. The radiation efficiency is only 26%–27% for the reference antenna, whereas the proposed design has doubled the efficiency to 53%–58%. Because both designs are almost equally matched,

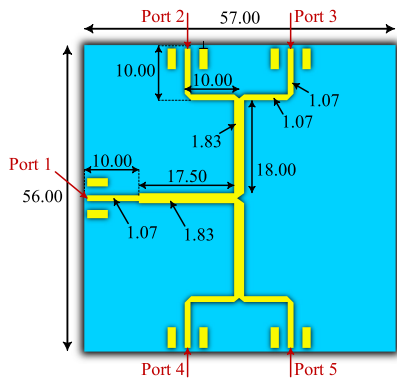


Fig. 5. Layout of the power divider. Port 1 is the feeding port, whereas other ports connect to the antenna ports. Dimensions are given in millimeters.

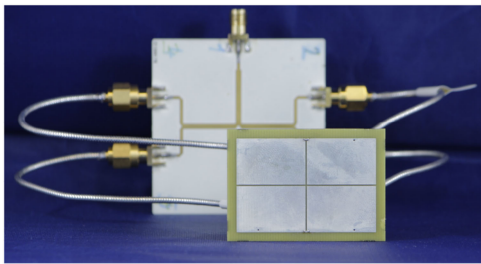


Fig. 6. Fabricated antenna (front) connected to the feeding network (back).

the improvement in total efficiency is nearly doubled as well. The reference and proposed antennas have total efficiencies of 19%–24% and 42%–52%, respectively.

For comparison, the theoretical maximum for the radiation efficiency from (6) is shown in the figure as well. If the optimal currents could be realized exactly the radiation efficiency would be 65%, but practical component values and impedance mismatch result in loss of efficiency.

### B. Measurements

The measurements were carried out using the MVG StarLab 6 GHz system in Aalto University. Since the proposed antenna is fed from multiple ports, a feeding network is designed and fabricated. The network consists of an equal four-way power divider designed on a 0.508 mm thick Rogers RO4350B substrate, and semirigid coaxial cables. The layout of the power divider is shown in Fig. 5. The  $180^\circ$  phase shift between the ports is implemented with semirigid coaxial cables by varying the cable length. Thus, the phase difference is exactly  $180^\circ$  between the shorter and longer cables at 2.45 GHz. The shorter and longer cables have lengths of 10 and 14.2 cm, respectively. The fabricated feeding network and antenna are shown in Fig. 6.

The total efficiency of the measured antenna, along with simulated efficiencies, is shown in Fig. 7. When the feeding network is introduced, the total efficiency is between 40%–48% for simulations and 33%–43% for measurements. The difference between simulations and measurements is due to additional

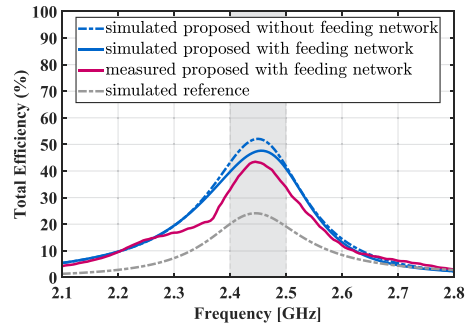


Fig. 7. Simulated total efficiencies of the reference antenna, and the proposed antenna with and without the feeding network. Also the measured total efficiency of the proposed antenna with the feeding network is shown.

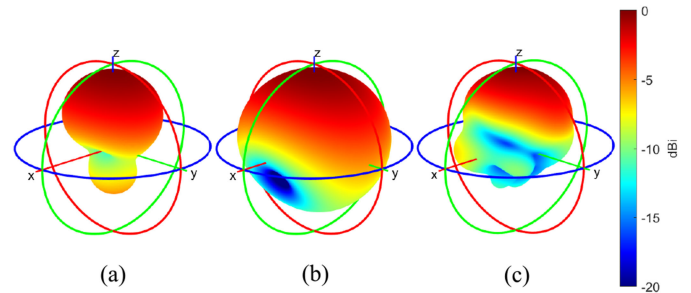


Fig. 8. Normalized radiation patterns of (a) the reference antenna, and (b) simulated and (c) measured proposed antenna with the feeding network included.

losses and asymmetries coming from the fabrication of the antenna and the feeding network.

Fig. 8 shows the normalized field patterns of the simulated reference antenna and the simulated and measured proposed antenna. The radiation patterns of the reference and proposed antennas are rather similar. Differences are that beamwidth in  $yz$  plane is larger for the proposed antenna, and the radiation to the back side is reduced by approximately 5 dB.

The results show that clear improvement can be achieved by finding an optimized design that is not necessarily the most obvious or intuitive. Similar conclusions can be drawn from a recent paper [24], where a dipole-like antenna was found to outperform a typical patch antenna of equivalent size.

### V. CONCLUSION

Realization of optimal currents for radiation efficiency is difficult for practical antennas. This letter took advantage of theoretical results and brought them computationally efficiently to practical design. The proposed method introduced a novel way to design antennas by maximizing radiation efficiency of a multifeed antenna. The simulated results showed that both the radiation and total efficiency were doubled as compared to a traditional reference case. The simulations were confirmed by measuring the multifeed antenna. The method enables a straightforward way for designing antennas, in environments where the traditional design lacks means to achieve sufficient radiation efficiency.



## REFERENCES

- [1] J. Kurvinen, A. Lehtovuori, J. Mai, C. Wang, and V. Viikari, "Metal-covered handset with LTE MIMO, Wi-Fi MIMO, and GPS antennas," *Prog. Electromagn. Res. C*, vol. 80, pp. 89–101, 2018.
- [2] K.-L. Wong, C.-C. Wan, and L.-Y. Chen, "Self-decoupled compact metal-frame LTE MIMO antennas for the smartphone," *Microw. Opt. Technol. Lett.*, vol. 60, no. 5, pp. 1170–1179, May 2018.
- [3] S. A. Ja'afreh, Y. Huang, and L. Xing, "Low profile and wideband planar inverted-F antenna with polarisation and pattern diversities," *Microw. Antennas Propag.*, vol. 10, no. 2, pp. 152–161, 2016.
- [4] Y. L. Ban, J. H. Chen, S. Yang, J. L. W. Li, and Y. J. Wu, "Low-profile printed octa-band LTE/WWAN mobile phone antenna using embedded parallel resonant structure," *IEEE Trans. Antennas Propag.*, vol. 61, no. 7, pp. 3889–3894, Jul. 2013.
- [5] L. Zhang, Y. Ban, C. Sim, J. Guo, and Z. Yu, "Parallel dual-loop antenna for WWAN/LTE metal-rimmed smartphone," *IEEE Trans. Antennas Propag.*, vol. 66, no. 3, pp. 1217–1226, Mar. 2018.
- [6] S. Song and R. D. Murch, "An efficient approach for optimizing frequency reconfigurable pixel antennas using genetic algorithms," *IEEE Trans. Antennas Propag.*, vol. 62, no. 2, pp. 609–620, Feb. 2014.
- [7] E. Hassan, E. Wadbro, and M. Berggren, "Topology optimization of metallic antennas," *IEEE Trans. Antennas Propag.*, vol. 62, no. 5, pp. 2488–2500, May 2014.
- [8] R. Li, D. McNamara, G. Wei, and J. Li, "Increasing radiation efficiency using antenna shape optimization approach," *IEEE Antennas Wireless Propag. Lett.*, vol. 17, no. 3, pp. 393–396, Mar. 2018.
- [9] S. Soltani, P. Lotfi, and R. D. Murch, "Design and optimization of multiport pixel antennas," *IEEE Trans. Antennas Propag.*, vol. 66, no. 4, pp. 2049–2054, Apr. 2018.
- [10] Optenni Ltd. Optenni Lab., 2019. [Online]. Available: <https://www.optenni.com/>
- [11] L. J. Chu, "Physical limitations of omni-directional antennas," *J. Appl. Phys.*, vol. 19, no. 12, pp. 1163–1175, Dec. 1948.
- [12] C. Pfeiffer, "Fundamental efficiency limits for small metallic antennas," *IEEE Trans. Antennas Propag.*, vol. 65, no. 4, pp. 1642–1650, Apr. 2017.
- [13] H. L. Thal, "Radiation efficiency limits for elementary antenna shapes," *IEEE Trans. Antennas Propag.*, vol. 66, no. 5, pp. 2179–2187, May 2018.
- [14] M. Shahpari and D. V. Thiel, "Fundamental limitations for antenna radiation efficiency," *IEEE Trans. Antennas Propag.*, vol. 66, no. 8, pp. 3894–3901, Aug. 2018.
- [15] M. Gustafsson, J. Fridn, and D. Colombi, "Antenna current optimization for lossy media with near-field constraints," *IEEE Antennas Wireless Propag. Lett.*, vol. 14, pp. 1538–1541, 2015.
- [16] M. Gustafsson and S. Nordebo, "Optimal antenna currents for Q, superdirectivity, and radiation patterns using convex optimization," *IEEE Trans. Antennas Propag.*, vol. 61, no. 3, pp. 1109–1118, Mar. 2013.
- [17] M. Gustafsson and B. L. G. Jonsson, "Antenna Q and stored energy expressed in the fields, currents, and input impedance," *IEEE Trans. Antennas Propag.*, vol. 63, no. 1, pp. 240–249, Jan. 2015.
- [18] C. Ehrenborg and M. Gustafsson, "Fundamental bounds on MIMO antennas," *IEEE Antennas Wireless Propag. Lett.*, vol. 17, no. 1, pp. 21–24, Jan. 2018.
- [19] L. Jelinek and M. Capek, "Optimal currents on arbitrarily shaped surfaces," *IEEE Trans. Antennas Propag.*, vol. 65, no. 1, pp. 329–341, Jan. 2017.
- [20] C. Li and R. Mittra, "Control of radiation patterns of antennas mounted on complex platforms by using the characteristic basis functions (CBFs)," *J. Electromagn. Waves Appl.*, vol. 30, no. 10, pp. 1354–1365, 2016.
- [21] R. Harrington, "Reactively controlled directive arrays," *IEEE Trans. Antennas Propag.*, vol. AP-26, no. 3, pp. 390–395, May 1978.
- [22] V. V. S. Prakash and R. Mittra, "Characteristic basis function method: A new technique for efficient solution of method of moments matrix equations," *Microw. Opt. Technol. Lett.*, vol. 36, no. 2, pp. 95–100, 2003.
- [23] S. Otto, S. Held, A. Rennings, and K. Solbach, "Array and multiport antenna farfield simulation using EMPIRE, MATLAB and ADS," in *Proc. Eur. Microw. Conf.*, Sep. 2009, pp. 1547–1550.
- [24] J. Singh, R. Stephan, and M. A. Hein, "Low-profile wideband differentially fed di-patch antenna closely above metallic ground," *IEEE Antennas Wireless Propag. Lett.*, vol. 18, no. 5, pp. 976–980, May 2019.